Metastable Perovskite $Bi_{1-x}La_xFe_{0.5}Sc_{0.5}O_3$ Phases in the Range of the Compositional Crossover

A.N. Salak[1*], D.D. Khalyavin[2#], I. Zamaraite[3] A. Stanulis[4], A. Kareiva[4], A.D. Shilin[5], V.V. Rubanik[5], Yu.V. Radyush[6], A.V. Pushkarev[6], N.M. Olekhnovich[6], M. Starykevich[1], R. Grigalaitis[3], M. Ivanov[3], J. Banys[3]

[1]Department of Materials and Ceramic Engineering and CICECO – Aveiro Institute of Materials, University of Aveiro, 3810-193 Aveiro, Portugal

[2]ISIS Facility, Rutherford Appleton Laboratory, Chilton, OX11 0QX Didcot, UK

[3]Faculty of Physics, Vilnius University, Sauletekio Street, 9-3, LT-10222 Vilnius, Lithuania

[4]Faculty of Chemistry, Vilnius University, Naugarduko Street, 24, LT-03225 Vilnius, Lithuania

[5]Institute of Technical Acoustics of NAS of Belarus, Lyudnikov Avenue, 13, 210023 Vitebsk, Belarus

[6]Scientific-Practical Materials Research Centre of NAS of Belarus, P. Brovka Street, 19, 220072 Minsk, Belarus

Abstract

Perovskite ceramics of the $Bi_{1-x}La_xFe_{0.5}Sc_{0.5}O_3$ composition ($0.30 \leq x \leq 0.35$) that cannot be sintered in bulk form as a single phase using the conventional ceramic route were successfully prepared using the high-pressure/high-temperature technique. It has been shown that the room-temperature compositional crossover from the antipolar phase whose incommensurate modulation of displacements of Bi/La and oxygen is described by the *Imma*(00γ)s00 superspace group to the non-polar *Pnma* phase occurs in the narrow range between x=0.33 and x=0.34 with no phase coexistence. The features of this compositional crossover are discussed in comparison with that observed in the $Bi_{1-x}La_xFeO_3$ system.

KEYWORDS: multiferroic, metastable phase, sol-gel method, high-pressure synthesis

* salak@ua.pt

dmitry.khalyavin@stfc.ac.uk

Introduction

Perovskite bismuth ferrite is one of the most studied multiferroics since this compound can be obtained using the conventional preparation methods. $BiFeO_3$ is ferroelectric until T_C=1083 K while the magnetic-paramagnetic phase transition occurs at T_N=643 K [1]. The temperatures of both transitions are too high and far from each other which makes difficult a beneficial use of the lattice-magnetic coupling effect. Moreover, in bulk $BiFeO_3$, the spins form a long-period cycloid that results in averaging of the local weak ferromagnetic components to zero [2]. A zero-field polar weak-ferromagnetic state in bismuth ferrite can be stabilized by means of chemical dopings. Besides, substitutions in the Bi^{3+} sites and in the Fe^{3+} sites modify the temperatures of the ferroelectric transition and the magnetic transition, respectively. A number of studies have been performed in this respect [3-6].

The $BiFeO_3$-based solid solution systems where bismuth is substituted by a rear earth element are the most explored (Ref [7] and references therein). Structural phases different from the parent rhombohedral *R*3*c* have been obtained and thoroughly studied [8-12]. Fe-site substitutions in bismuth ferrite are much less investigated since, in the majority of cases, small substitution rates (an order of 10 mol% when the resulting structure is still rhombohedral) are only achievable. As a rule, non-conventional preparation methods are needed to obtain the extended (entire) solid solution systems with substitution either in Fe^{3+} sites or in both cation sites. Polycrystalline solid solutions $Bi(Fe,B^{3+})O_3$ where B^{3+} is Co, Ga, Mn, Cr, Sc were prepared using the high-pressure/high-temperature method [13-18].

Recently, we initiated a systematic study of the quasi quadruple $BiFeO_3$–$BiScO_3$–$LaFeO_3$–$LaScO_3$ perovskite system. Three end members of this system, $BiFeO_3$, $LaFeO_3$ and $LaScO_3$, can be obtained using the conventional methods (in particular, the standard ceramic technique), while a bulk perovskite $BiScO_3$ phase can be synthesized under the high-pressure conditions only [19]. The main idea of the exploration of the $Bi_{1-x}La_xFe_{1-y}Sc_yO_3$ system is to control (adjust) the temperatures of the magnetic and the polar transitions. In this system, all the constituent cations are trivalent that makes possible to vary the parameters *x* and *y* independently. Hence, one can decrease the temperature of polar transition by means of a replacement of bismuth by lanthanum and decrease the temperature of magnetic transition through an iron-to-scandium substitution. Therein, the purpose of this study was to obtain the solid solution with the overlapping ranges of T_C and T_N aiming to achieve the maximal lattice-magnetic coupling effect.

We have reported three different structural phases observed in the as-prepared polycrystalline samples of the particular section of the system, when the Fe/Sc ratio is fixed to be 1:1. At room temperature, the perovskite phase of the $Bi_{1-x}La_xFe_{0.5}Sc_{0.5}O_3$ ceramics with x=0 was

found to be antipolar *Pnma* with the $\sqrt{2}a_p \times 4a_p \times 2\sqrt{2}a_p$ superstructure (a_p is the pseudocubic unit cell) [20]. In the ceramics with the x=0.20 composition, an incommensurate modulation of displacements of Bi/La and oxygen is described by the *Imma*(00γ)s00 superspace group ($\sqrt{2}a_p \times 2a_p \times \sqrt{2}a_p$) [21]. Non-polar *Pnma* phase ($\sqrt{2}a_p \times 2a_p \times \sqrt{2}a_p$) was detected in the samples with x=0.35 [22]. In all the mentioned compositions, the magnetic transition was observed at about 220 K [20-24], i.e. slightly below room temperature. Below T_N, these solid solutions were shown to exhibit long-range antiferromagnetic ordering with a weak ferromagnetic component.

Neutron diffraction study of the $Bi_{1-x}La_xFe_{0.5}Sc_{0.5}O_3$ ceramics with x=0.35 performed between room temperature and 1.5 K has revealed no transition from the non-polar *Pnma* phase [22]. Thus, at room temperature, the solid solution with x=0.20 is an antipolar while that with x=0.35 is a non-polar. Hence, the composition of the solid solution whose transition between the antipolar phase and non-polar phase occurs in the vicinity of room temperature is certainly between 0.20 and 0.35.

In this work, the $Bi_{1-x}La_xFe_{0.5}Sc_{0.5}O_3$ solid solutions in the range of $0.30 \leq x \leq 0.35$ were prepared and thoroughly investigated aiming at determination of the compositional phase crossover and identify the composition for which T_C is close to T_N. The ceramics were synthesized/sintered under high pressure. The obtained samples were characterized using the methods of x-ray diffraction (including *in situ* temperature XRD) and dielectric spectroscopy. The features of this compositional crossover are discussed in comparison with that observed in the $Bi_{1-x}La_xFeO_3$ system.

Experimental

High-purity Bi_2O_3, La_2O_3, Fe_2O_3, and Sc_2O_3 were used as starting reagents to prepare the $Bi_{1-x}La_xFe_{0.5}Sc_{0.5}O_3$ compositions with x=0.30 and 0.35. Previously calcined oxides were mixed in the stoichiometric ratio, ball milled in acetone, dried, and pressed into pellets. The pellets were heated in a closed alumina crucible at 1140 K for 10 min followed by a quenching down to room temperature to be then used for the high-pressure synthesis/sintering.

Since the crystal structure of the $Bi_{1-x}La_xFe_{0.5}Sc_{0.5}O_3$ phases is certainly very sensitive to x, it is a fundamental issue to ensure the proper chemical composition in the precursors and, thereby, in the ceramics. The sol-gel method is known to offer opportunity to obtain ultra-homogeneous complex oxide materials. Therefore, the $Bi_{1-x}La_xFe_{0.5}Sc_{0.5}O_3$ precursors (x=0.30-0.35, step 0.01) were also prepared *via* a sol-gel combustion route using nitrates of the respective metals. The appropriate volumes of the nitrates were mixed together in a beaker and complexing agent (citric acid monohydrate) was then added to the above solution in different molar ratios

according to propellant chemistry. The resulted solution was mixed for 1 h at 333 K and then concentrated by evaporation of solvent at 373 K until it turned into a brown viscous gel. Finally, the resulted gel was heated up to about 670 K to initiate combustion reaction. The obtained ultra-fine powders were calcined in air at 870 K for 2 h to remove organic remains. High-power sonication of the powders was performed in ethanol in the cavitation regime using a water cooled 30-ml cell. The ultrasonic generator power was 0.5 kW, the treatment time was 20 min. The dried powder was pressed into pellets and used for the high-pressure synthesis/sintering without any additional thermal treatment.

High pressure was generated using an anvil press DO-138A with a press capacity up to 6300 kN. The ceramic samples were prepared at 6 GPa for 1-2 min. In order to produce ceramics from the thermally treated mixture of oxides, one needed the synthesis/sintering temperature to be in the range of 1420-1520 K, while in case of the sol-gel prepared precursor the temperature of 1020-1120 K was enough.

Powder XRD study of the precursors and the sintered samples was performed using a PANalytical XPert MPD PRO diffractometer (Ni-filtered Cu$K\alpha$ radiation, PIXcel^{1D} detector, and the exposition corresponded to about 2 s per step of 0.02^{o} over the angular range of 15-100^{o}) at room temperature. *In situ* XRD measurements were conducted in an Anton Paar high-temperature chamber (HTK 16N) in a temperature range between 300 K and 870 K. Rietveld refinements of the diffraction data have been performed using JANA 2006 software [25]. For the x=0.35 composition, the room temperature structural parameters were refined from both X-ray and neutron diffraction data (see Ref. [22] for details of the neutron diffraction experiment) revealing their excellent agreement.

The microstructure of the fractured surface and local chemical composition of the obtained ceramics was studied by scanning electron microscopy (SEM, Hitachi S-4100) equipped with an energy dispersive spectroscopy (EDS) detector.

Dielectric measurements were performed in the temperature range of 100-500 K and at frequencies from 20 Hz to 2 GHz using an LCR meter (HP 4284A) and a Vector Network Analyser (Agilent 8714ET). The ceramic samples were polished to obtain discs of about 0.5 mm thick and then electroded with silver paste.

Results and Discussion

Attempts to prepare a single-phase $Bi_{1-x}La_xFe_{0.5}Sc_{0.5}O_3$ perovskite solid solution with x=0.30 using the conventional ceramic route were unsuccessful. Two main phases were detected in the product of thermal treatment of the stoichiometric mixture of oxides, namely a perovskite phase derived from $BiFeO_3$ with the rhombohedral distortion of the crystal lattice and a phase based on either γ- or β- modifications of Bi_2O_3 (depending on the treatment temperature) [18]. Direct synthesis under high pressure from the oxide mixture without thermal treatment has resulted in no single-phase product: along with the perovskite phase, a monoclinic phase based on bismuth oxide was present [18]. Single-phase perovskite ceramics with x=0.30 have been prepared by means of high-pressure synthesis/sintering of the thermally treated oxide mixture as indicated in *Experimental*.

It has been found from the analysis of the XRD pattern of these ceramics that the symmetry of the as-prepared phase with x=0.30 is the same as that of the phase with x=0.20, namely an incommensurately modulated antipolar phase that can be described using the *Imma*(00γ)s00 superspace group [21]. Thus, the range of interest can be specialized: in the $Bi_{1-x}La_xFe_{0.5}Sc_{0.5}O_3$ system, the crossover from antipolar to non-polar phase occurs in the range between x=0.30 and 0.35. The compositional behaviour of the normalized unit-cell volume in this range suggests likely structural transition: the volume value drops by about 0.8%; i.e., by 1.6% per step of Δx=0.10. Cf: in the range of x between 0.20-0.30 where the solid solutions remain antipolar, the observed decrease of the volume is as small as about 0.4% per the same step.

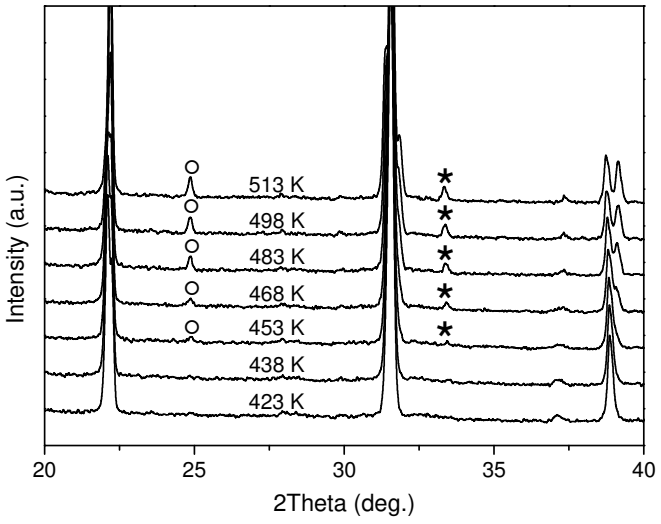

Figure 1. XRD patterns of the $Bi_{0.7}La_{0.3}Fe_{0.5}Sc_{0.5}O_3$ samples at different temperatures (on heating) below and above the transition between the antipolar and non-polar perovskite phases. Reflections (111) and (210) of the non-polar *Pnma* phase are marked with open cycles and asterisks, respectively.

In situ XRD study has revealed that the antipolar phase of the $Bi_{1-x}La_xFe_{0.5}Sc_{0.5}O_3$ solid solution with x=0.30 transforms on heating into the non-polar *Pnma* phase which is similar to that detected in the as-prepared samples of the x=0.35 composition [22]. The transformation was found to be reversible. On heating, the *Imma*(00γ)s00→*Pnma* transition begins at about 450 K; on cooling, the *Pnma*→*Imma*(00γ)s00 transition is complete at about 440 K. Beginning (ending) of the transition was determined by appearance (disappearance) of the weak commensurate reflections (111) and (210) characteristic of the non-polar phase (Figure 1).

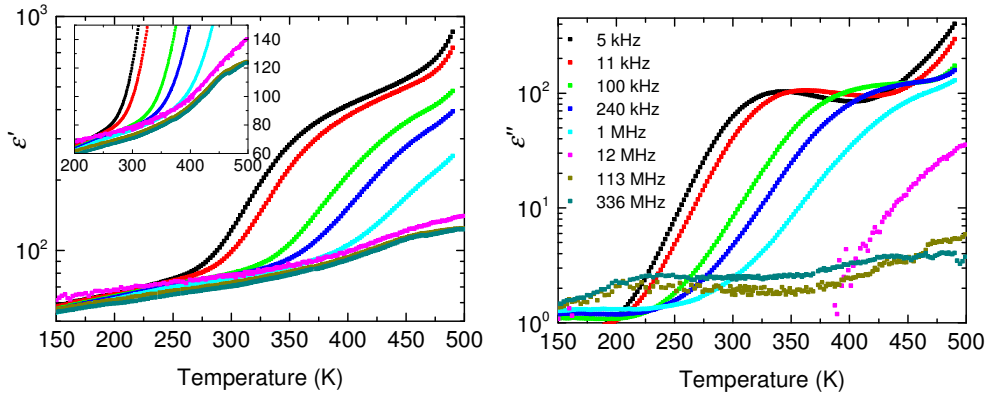

Figure 2. Temperature dependence of the real (*left*) and the imaginary (*right*) parts of complex dielectric permittivity of the $Bi_{0.7}La_{0.3}Fe_{0.5}Sc_{0.5}O_3$ ceramic sample at selected frequencies.

Dielectric measurements confirmed the transition in the ceramics with the x=0.30 composition (Figure 2). The obtained temperature dependences of complex dielectric permittivity for $Bi_{0.7}La_{0.3}Fe_{0.5}Sc_{0.5}O_3$ exhibit anomalous behavior at about 460 K, clearly visible at frequencies above 20 MHz. This anomaly is associated with the antipolar-nonpolar phase transition which was observed in the *in situ* XRD study. At lower frequencies, rather high dielectric losses indicate contribution of conductivity and no polar nature of the material can be observed.

It is well known that the materials based on $BiFeO_3$ are characterized by a high loss caused by the electronic structure of this compound (intrinsic loss). However, in our ceramics, an extrinsic contribution to the loss, i.e. loss associated with the microstructure is certainly considerable. It was found from the high-pressure experiments that homogeneous ceramics of the satisfactory quality can be prepared only in a very narrow temperature range. When the synthesis/sintering temperature is not high enough, the obtained material is very porous and poorly sintered. Application of the temperature that exceeds the range results in formation of a considerable amount of liquid phase in which the big grains grow up.

Typical microstructure of the fractured surface of the high-pressure prepared ceramics is shown in Figure 3a. The relatively thick intergranular layers and the gaps between the grains are seen.

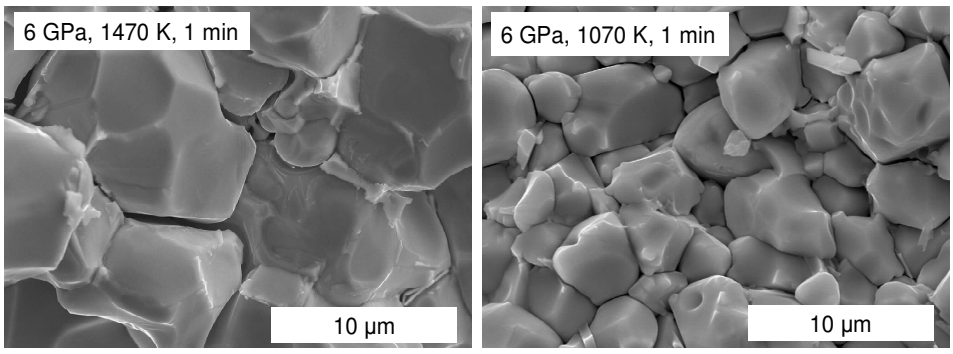

Figure 3. SEM images of the fractured surfaces of the $Bi_{1-x}La_xFe_{0.5}Sc_{0.5}O_3$ ceramics (x=0.30) synthesized/sintered under high pressure (a) from a mechanical mixture of the respective oxides and (b) from the powders prepared using a sol-gel combustion route.

In order to produce more homogeneous and dense ceramics at lower synthesis/sintering temperature, the advanced methods of precursor preparation were used. XRD analysis of the $Bi_{1-x}La_xFe_{0.5}Sc_{0.5}O_3$ powders with x from 0.30 to 0.35 (step 0.01) prepared using the sol-gel (combustion) method followed by annealing at 870 K revealed that the perovskite phase is the only phase present. However, it was impossible to determine the symmetry of the phase since the diffraction peaks were broadened (Figure 4). This broadening can be caused either by poor crystallization or small crystallite size.

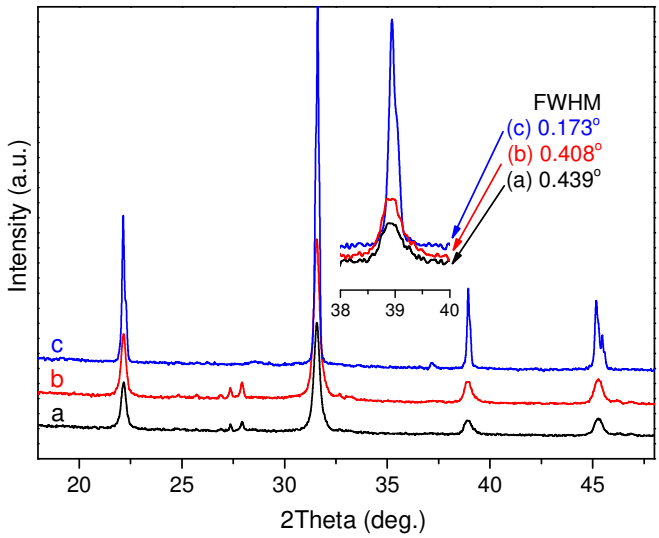

Figure 4. XRD patterns of the $Bi_{1-x}La_xFe_{0.5}Sc_{0.5}O_3$ powders with x=0.32 prepared using the sol-gel (combustion) route and annealed at 600°C: (a) as-prepared, (b) sonicated at 0.5 kW for 20 min, and (c) synthesized/sintered at 6 GPa and 800°C for 1 min. Insert shows the range of the (220)/(022) diffraction peak and the respective values of the full width at half maximum (FWHM).

It was found that a high-power sonication of the sol-gel prepared powders has a positive effect: the diffraction reflections of the perovskite phase became sharper and better resolved. Such an effect suggests that the observed peak broadening should be associated with poor

(incomplete) crystallization rather than with small size of the crystallites. High-power sonication (which is a kind of mechanoactivation) certainly promotes further crystallization of the sol-gel prepared powders. This phenomena deserves a particular study which is out of the scope of this paper. Although the obtained powders were single-phase perovskite, the attempts to sinter them into homogeneous ceramics under ambient pressure were unsuccessful. Different sintering temperatures above 870 K were tested; however, the obtained product was either not sintered or a non-single phase. The sintered material was found to have a similar phase composition as the product of synthesis from the mechanical oxide mixture (as mentioned at the beginning of *Results and Discussion*).

It turned out that the powders obtained through a sol-gel route followed by a high-power sonication can be sintered into single-phase ceramics under high pressure at the temperatures that are 300-400 K lower that those applied when preparing ceramics from the thermally treated mixed oxide precursors. Comparison of XRD patterns showed that the perovskite phases of the ceramic samples of the same nominal composition (with either x=0.30 or x=0.35, see *Experimental*) are identical in terms of crystallinity and the lattice parameters in spite of both different ways of the precursor preparations and different temperatures of the high-pressure treatment. However, the ceramics produced from the sol-gel prepared precursors was found to be more homogeneous and denser: with thinner intergranular layers and smaller gaps between the grains (cf. Figure 3a and Figure 3b). An EDS mapping revealed a more homogeneous distribution of iron and scandium over the grains and the intergranular layers.

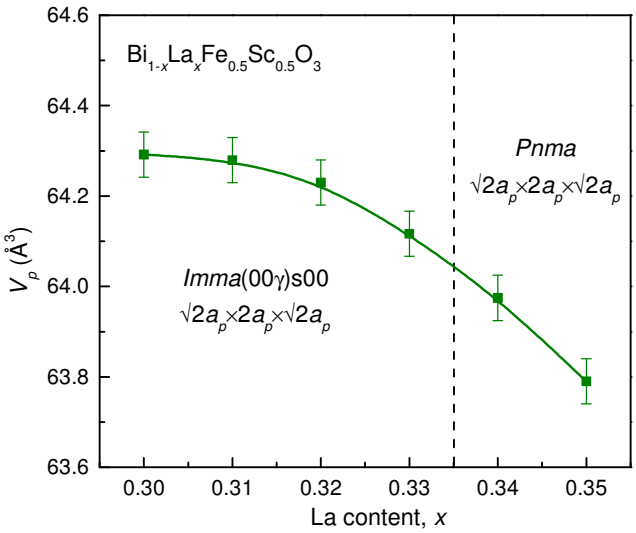

Figure 5. The normalized unit-cell volume of the $Bi_{1-x}La_xFe_{0.5}Sc_{0.5}O_3$ perovskite phases at room temperature as a function of the lanthanum content in the compositional range of $0.30 \le x \le 0.35$. Dashed line shows the tentative border between the antipolar phase and the non-polar phases at room temperature.

It was found from the analysis of the XRD patterns of these ceramics that the $Bi_{1-x}La_xFe_{0.5}Sc_{0.5}O_3$ perovskite phase is an incommensurate antipolar *Imma*(00γ)s00 when $x \leq 0.33$ and a non-polar *Pnma* when $x \geq 0.34$. Figure 5 shows the compositional dependence of the normalized unit cell volume in the range from 0.30 to 0.35. No region of phase coexistence has been detected. In this respect, the composition-phase behaviour of the $Bi_{1-x}La_xFe_{0.5}Sc_{0.5}O_3$ perovskite solid solutions in the range of crossover from antipolar phase to non-polar one is a striking departure from that generally observed in the perovskite systems derived from bismuth ferrite. The $BiFeO_3$-based solid solution systems where bismuth is substituted by a rear earth element demonstrate a wide-range phase coexistence at the antipolar-to-non-polar compositional crossover [26-28]. Particularly, in the $Bi_{1-x}La_xFeO_3$ system, such a crossover occurs over the range of at least 10 mol% [29]. Although the lanthanum-substituted $BiFeO_3$ perovskites are the most studied among the system based on bismuth ferrite, there are several different opinions on nature of coexisting phases in this range [26,29-34]. Overlapped diffraction peaks in XRD patterns result in difficulties/ uncertainties in identification of the phases.

The energy landscape of $BiFeO_3$-based compositions consists of several almost degenerate phase states. That is why a phase coexistence is typical of these materials. However, the phase states can be switched by some perturbations. We assume that pressure acts as such a perturbation and makes the composition-phase dependence more certain. The $Bi_{1-x}La_xFe_{0.5}Sc_{0.5}O_3$ phases were obtained by means of sintering under high pressure followed a quenching down to room temperature. It appears that under pressure a difference in energies of the phases with different symmetries is more noticeable and one phase or another becomes certainly more favourable.

Detailed dielectric study and investigation of the magneto-electric effect in the $Bi_{1-x}La_xFe_{0.5}Sc_{0.5}O_3$ ceramics with $0.30 \leq x \leq 0.35$ are in progress and will be published elsewhere.

Conclusions

Single-phase perovskite ceramics of the $Bi_{1-x}La_xFe_{0.5}Sc_{0.5}O_3$ composition ($0.30 \leq x \leq 0.35$) cannot be prepared using a conventional mixed oxide route. A thermal treatment at ambient pressure of a stoichiometric mixture of the respective oxides results in formation of a $BiFeO_3$-like rhombohedral perovskite and a phase based on the polymorphic modifications of Bi_2O_3.

$Bi_{1-x}La_xFe_{0.5}Sc_{0.5}O_3$ powders ($0.30 \leq x \leq 0.35$) prepared using the sol-gel combustion method followed by calcination are single-phase although poorly crystallized. High-power sonication of the powders was found to promote further crystallization. This phenomenon deserves a particular study. However, regardless of the precursor preparation method (either from the thermally

treated oxide mixture or from the sol-gel derived powders), in order to sinter single-phase ceramics from these powders, the high-pressure/high-temperature technique is needed. At the same time, the powders obtained through a sol-gel route can be sintered into single-phase ceramics under high pressure at the temperatures that are 300-400 K lower that those applied when preparing ceramics from the thermally treated mixed oxide precursors.

The compositional crossover from the incommensurately modulated antipolar phase that can be described using the *Imma*(00γ)s00 superspace group to the non-polar *Pnma* phase in the $Bi_{1-x}La_xFe_{0.5}Sc_{0.5}O_3$ system at room temperature occurs between x=0.33 and 0.34 with no range of phase coexistence. This very narrow compositional range is of a great interest since it corresponds to a solid solution with the maximal lattice-magnetic coupling effect expected.

Acknowledgement

This work was supported by project TUMOCS. This project has received funding from the European Union's Horizon 2020 research and innovation programme under the Marie Skłodowska-Curie grant agreement No 645660. Financial support of the Belarusian Republican Foundation for Fundamental Research (Project No T15VT-008) is gratefully acknowledged as well.

References

1. Catalan G, Scott JF. Physics and applications of bismuth ferrite. *Adv. Mater.* 2009; **21**: 2463-2485.
2. Sosnowska I, Neumaier TP, Steichele E. Spiral magnetic ordering in bismuth ferrite. *J. Phys. C*. 1982; **15**: 4835-4846.
3. Jun YK, Lee SB, Kim M, Honga SH, Kim JW, Kim KH. Dielectric and magnetic properties in Ta-substituted $BiFeO_3$ ceramics. *J. Mater. Res*., 22, 2007 3397-3403.
4. Wu H, Lin YB, Gong JJ, Zhang F, Zeng M, Qin MH, Zhang Z, Ru Q, Liu ZW, Gao XS, Liu, JM. Significant enhancements of dielectric and magnetic properties in $Bi(Fe_{1-x}Mg_x)O_{3-x/2}$ induced by oxygen vacancies. *J. Phys. D: Appl. Phys*. 2013; **46**: Art. No 145001.
5. Kumar P, Kar, M. Tuning of net magnetic moment in $BiFeO_3$ multiferroics by co-substitution of Nd and Mn. *Physica B*. 2014; **448**: 90-95.
6. Khomchenko VA, Paixaõ, JA. Ti doping-induced magnetic and morphological transformations in Sr- and Ca-substituted $BiFeO_3$. *J. Phys.: Condens. Matter* 2016; **28**: Art. No166004.
7. Arnold DC. Composition-driven structural phase transitions in rare-earth-doped $BiFeO_3$ ceramics: a review. *IEEE Trans. Ultrasonics. Ferroelectrics. Freq. Control.* 2015; **62**: 62-82.
8. Khomchenko VA, Paixaõ JA, Shvartsman VV, Borisov P, Kleemann W, Karpinsky DV, Kholkin AL. Effect of Sm substitution on ferroelectric and magnetic properties of $BiFeO_3$. *Scr. Mater*. 2010; **62**: 238-241.
9. Karpinsky DV, Troyanchuk IO, Sikolenko V, Efimov V, Efimova E, Willinger M, Salak AN, Kholkin AL. Phase coexistence in $Bi_{1-x}Pr_xFeO_3$ ceramics. *J. Mater. Sci.* 2014; **49**: 6937-6943.
10. Suresh P, Babu PD, Srinath S. Effect of Ho substitution on structure and magnetic properties of $BiFeO_3$. *J. Appl. Phys*. 2014; **115**: Art. No 17D905.
11. Kumar A, Varshney D. Structural transition and enhanced ferromagnetic properties of La, Nd, Gd, and Dy-doped $BiFeO_3$ ceramics. *J. Electron. Mater*. 2015; **44**: 4354-4366.
12. Muneeswaran M, Dhanalakshmi R, Giridharan NV. Effect of Tb substitution on structural, optical, electrical and magnetic properties of $BiFeO_3$. *J. Mater. Sci. Mater. Electron*. 2015; **26**: 3827-3839.
13. Azuma M, Kanda, Belik AA, Shimakawa Y, Takano M. Magnetic and structural properties of $BiFe_{1-x}Mn_xO_3$. *J. Magn. Magn. Mater*. 2007; **310**: 1177-1179.
14. Azuma M, Niitaka S, Hayashi N, Oka K, Takano M, Funakubo H, Shimakawa Y. Rhombohedral-tetragonal phase boundary with high curie temperature in $(1-x)BiCoO_3$–$xBiFeO_3$ solid solution. *Jpn. J. Appl. Phys*. 2008; **47**: 7579-7581.

15. Kubota M, Oka K, Yabuta H, Miura K, Azuma M. Structure and magnetic properties of $BiFe_{1-x}Co_xO_3$ and $Bi_{0.9}Sm_{0.1}Fe_{1-x}Co_xO_3$, *Inorg. Chem.* 2013; **52**:10698-10704.

16. Belik AA, Rusakov DA, Furubayashi T, Takayama-Muromachi E. $BiGaO_3$-based perovskites: a large family of polar materials, *Chem. Mater.* 2012; **24**: 3056-3064.

17. Suchomel MR, Thomas CI, Allix M, Rosseinsky MJ, Fogg AM, Thomas MF. High pressure bulk synthesis and characterization of the predicted multiferroic $Bi(Fe_{1/2}Cr_{1/2})O_3$. *Appl. Phys. Lett.* 2007; **90**: Art. No 112909.

18. Salak AN, Khalyavin DD, Pushkarev AV, Radyush YuV, Olekhnovich NM, Shilin AD, Rubanik VV. Phase formation in the $(1-y)BiFeO_3$-$yBiScO_3$ system under ambient and high pressure. *J. Solid State Chem.* 2017; **247**: 90-96.

19. Belik AA, Iikubo S, Kodama K, Igawa N, Shamoto S, Maie M, Nagai T, Matsui Y, Stefanovich SYu, Lazoryak BI, Takayama-Muromachi E. $BiScO_3$: centrosymmetric $BiMnO_3$-type oxide. *J. Amer. Chem. Soc.* 2006; **128**: 706-707.

20. Khalyavin DD, Salak AN, Olekhnovich NM, Pushkarev AV, Radyush YuV, Manuel P, Raevski IP, Zheludkevich ML, Ferreira MGS. Polar and antipolar polymorphs of metastable perovskite $BiFe_{0.5}Sc_{0.5}O_3$. *Phys. Rev. B.* 2014; **89**: Art. No 174414.

21. Khalyavin DD, Salak AN, Lopes AB, Olekhnovich NM, Pushkarev AV, Radyush YuV, Fertman EL, Desnenko VA, Fedorchenko AV, Manuel P, Feher A, Vieira JM, Ferreira MGS. Magnetic structure of an incommensurate phase of La-doped $BiFe_{0.5}Sc_{0.5}O_3$: role of antisymmetric exchange interactions. *Phys. Rev. B.* 2015; **92**: Art. No 224428.

22. Khalyavin DD, Salak AN, Manuel P, Olekhnovich NM, Pushkarev AV, Radyush YuV, Fedorchenko AV, Fertman EL, Desnenko VA, Ferreira MGS. Antisymmetric exchange in La-substituted $BiFe_{0.5}Sc_{0.5}O_3$ system: symmetry adapted distortion modes approach. *Z. Kristallogr. Cryst. Matter.* 2015; **230**: 767-774.

23. Fertman EL, Fedorchenko AV, Khalyavin DD, Salak AN, Baran A, Desnenko VA, Kotlyar OV, Čižmár E, Feher A, Syrkin ES, Vaisburd AI, Olekhnovich NM, Pushkarev AV, Radyush YuV, Stanulis A, Kareiva A. Multiferroic $Bi_{0.65}La_{0.35}Fe_{0.5}Sc_{0.5}O_3$ perovskite: magnetic and thermodynamic properties. *J. Magn. Magn. Mater.* 2017; **429**: 177-181.

24. Fedorchenko AV, Fertman EL, Desnenko VA, Kotlyar OV, Čižmár E, Shvartsman VV, Lupascu DC, Salamon S, Wende H, Salak AN, Khalyavin DD, Olekhnovich NM, Pushkarev AV, Radyush YuV, Feher A. Magnetic properties of the $Bi_{0.65}La_{0.35}Fe_{0.5}Sc_{0.5}O_3$ perovskite. *Acta Physica Polonica A.* 2017 – *in press*.

25. Petříček V, Dušek M, Palatinus L, Crystallographic computing system JANA2006: General features, *Z. Kristallogr. Cryst. Mater.* 2014; **229**: 345-352.

26. Troyanchuk IO, Bushinsky MV, Karpinsky DV, Mantyskaya OS, Fedotova VV, Prokhnenko OI. Structural transformations and magnetic properties of $Bi_{(1-x)}Ln_{(x)}FeO_3$ (Ln = La, Nd, Eu). *Phys. Stat. Solidi B*. 2009; **246**: 1901-1907.

27. Khomchenko VA, Karpinsky DV, Kholkin AL, Sobolev NA, Kakazei GN, Araujo JP, Troyanchuk IO, Costa BFO, Paixão JA. Rhombohedral-to-orthorhombic transition and multiferroic properties of Dy-substituted $BiFeO_3$. *J. Appl. Phys.* 2010; **108**: Art. No 074109.

28. Karpinsky DV, Troyanchuk IO, Sikolenko V, Efimov V, Efimova E, Willinger M, Salak AN, Kholkin AL. Phase coexistence in $Bi_{1-x}Pr_xFeO_3$ ceramics. *J. Mater. Sci.* 2014; **49**: 6937-6943.

29. Rusakov DA, Abakumov AM, Yamaura K, Belik AA, Van Tendeloo G, Takayama-Muromachi E. Structural evolution of the $BiFeO_3$-$LaFeO_3$ system. *Chem. Mater.* 2011; **23**: 285-292.

30. Yuan GL, Or SW, Chan HLW. Structural transformation and ferroelectric-paraelectric phase transition in $Bi_{1-x}La_xFeO_3$ (x = 0-0.25) multiferroic ceramics. *J. Phys. D*. 2007; **40**: 1196-1200.

31. Cheng ZX, Li AH, Wang XL, Dou SX, Ozawa K, Kimura H, Zhang SJ, Shrout TR. Structure, ferroelectric properties, and magnetic properties of the La-doped $BiFeO_3$. *J. Appl. Phys*. 2008; **103**: Art. No 07E507.

32. Troyanchuk IO, Karpinsky DV, Bushinsky MV, Khomchenko VA, Kakazei GN, Araujo JP, Tovar M, Sikolenko V, Kholkin AL. Isothermal structural transitions, magnetization and large piezoelectric response in $Bi_{1-x}La_xFeO_3$ perovskites. *Phys. Rev. B*. 2011; **83**: Art. No 054109.

33. Le Bras G, Bonville P, Colson D, Forget A, Genand-Riondet N, Tourbot R. Effect of La doping in the multiferroic compound $BiFeO_3$. *Physica B*. 2011; **406**: 1492-1495.

34. Gonzalez-Vazquez OE, Wojdel JC, Dieguez O, Iniguez J. First principles investigation of the structural phases and enhanced response properties of the $BiFeO_3$-$LaFeO_3$ multiferroic solid solution. *Phys. Rev. B* 2012; **85**: Art. No 064119.